The MIR34B/C genomic region contains multiple potential regulators of multiciliogenesis

Amélie Cavard, Elisa Redman, Olivier Mercey, Sophie Abelanet, Magali
Plaisant, Marie-jeanne Arguel, Virginie Magnone, Sandra Ruiz García,
Géraldine Rios, Marie Deprez, et al.

The *MIR34B/C* genomic region contains multiple potential regulators of multiciliogenesis

Amélie Cavard[1], Elisa Redman[1], Olivier Mercey[2], Sophie Abelanet[1], Magali Plaisant[1], Marie-Jeanne Arguel[1], Virginie Magnone[1], Sandra Ruiz García[1], Géraldine Rios[1], Marie Deprez[1], Kévin Lebrigand[1], Gilles Ponzio[1], Ignacio Caballero[3], Pascal Barbry[1], Laure-Emmanuelle Zaragosi[1] and Brice Marcet[1]

1 Université Côte d'Azur, CNRS, IPMC, Sophia-Antipolis, France
2 Institut de Biologie de l'École Normale Supérieure, Paris, France
3 ISP, INRA, Université Tours, Nouzilly, France

Correspondence

L.-E. Zaragosi and B. Marcet, IPMC-CNRS, UMR-7275, 660 Route des Lucioles, 06560 Sophia-Antipolis, Valbonne, France
Tel: +33 (0)4 93 95 77 03
E-mail: zaragosi@ipmc.cnrs.fr (L-EZ); marcet@ipmc.cnrs.fr (BM)

Laure-Emmanuelle Zaragosi and Brice Marcet contributed equally to this article

The *MIR449* genomic locus encompasses several regulators of multiciliated cell (MCC) formation (multiciliogenesis). The miR-449 homologs miR-34b/c represent additional regulators of multiciliogenesis that are transcribed from another locus. Here, we characterized the expression of *BTG4*, *LAYN*, and *HOATZ*, located in the *MIR34B/C* locus using single-cell RNA-seq and super-resolution microscopy from human, mouse, or pig multiciliogenesis models. *BTG4*, *LAYN*, and *HOATZ* transcripts were expressed in both precursors and mature MCCs. The Layilin/LAYN protein was absent from primary cilia, but it was expressed in apical membrane regions or throughout motile cilia. *LAYN* silencing altered apical actin cap formation and multiciliogenesis. HOATZ protein was detected in primary cilia or throughout motile cilia. Altogether, our data suggest that the *MIR34B/C* locus may gather potential actors of multiciliogenesis.

Keywords: BTG4; HOATZ; LAYN; miR-34b/c; motile cilia; multiciliated cells

The airway epithelium is the first line of defense of airways against external stress and is constituted by several cell types including basal, club, goblet, and multiciliated cells (MCCs), as well as rare cells such as ionocytes [1-3]. MCCs carry hundreds of motile cilia at their apical surface which orchestrate mucociliary clearance [4,5]. Ciliary disorders are observed in ciliopathies and chronic respiratory diseases [4]. The formation of MCCs (a process called multiciliogenesis) requires the production of tens to hundreds of centrioles in a shallow time window, mostly through a structure named the deuterosome, composed, in part, by DEUP1 proteins [5,6]. Neosynthesized centrioles migrate apically to dock at the plasma membrane to initiate cilium elongation [5]. Over the last decade, the complex mechanisms underlying multiciliogenesis have begun to be unraveled.

Abbreviations

Ac. Tub., acetylated alpha-tubulin; ALI, air–liquid interface; APC/C, anaphase-promoting complex/cyclosome; BEBM, bronchial epithelial cell basal medium; BEGM, bronchial epithelial cell growth medium; BTG, B-cell translocation gene; Cas9, CRISPR-associated protein 9; CCNO, cyclin O; CDC20B, cell division cycle protein 20 homolog B; CRISPR, clustered regularly interspaced short palindromic repeats; DAPI, 4′,6-diamidino-2-phenylindole; DEUP1, deuterosome assembly protein 1; ENO4, enolase 4; FOXJ1, forkhead box J1; GAPDH, glyceraldehyde-3-phosphate dehydrogenase; HBEC, human bronchial epithelial cell; HNEC, human nasal epithelial cell; HOATZ, hydrocephalus and oligo-astheno-terato-zoospermia; IFT, intraflagellar transport; LAYN, Laylin; MCC, multiciliated cell; MCIDAS, multiciliate differentiation and DNA synthesis associated cell cycle protein; MiRNA or miR, microRNA; mTEC, mouse tracheal epithelial cell; PLK1, polo-like kinase 1; RhoA, Ras homolog family member A; ROCK, Rho-associated, coiled-coil-containing protein kinase; scRNA-seq, single-cell RNA-sequencing; siRNA, small interfering RNA; SNTN, Sentan; STED, stimulated emission depletion; UMI, unique molecular identifier.

Multiciliogenesis involves a coordinated expression of hundreds of genes. Some, such as *MCIDAS*, *CCNO*, *CDC20B*, and *MIR449A/B/C*, are located in the same evolutionarily conserved genomic locus (5q11 in human) and all participate in multiciliogenesis [7-9]. This complementary contribution of genes located in the same locus in the same biological process led us to propose that this locus acts as a 'multiciliary locus' [9]. The miR-34/449 microRNA (miRNA or miR) superfamily, largely conserved across vertebrates, is encoded by six miRNA genes located in three distinct loci: (a) *MIR449A/B/C* are located in the second intron of the host gene *CDC20B* (5q11 in human) [8-10], (b) *MIR34B/C* are located on a second conserved locus between *C11orf88* and *BTG4* (11q23 in human), (c) *MIR34A* is located on a third locus (1p36 in human) [8,10]. Whereas miR-34a seems to be the only member of the family that has not been associated with MCC differentiation, we and others have previously described the role of miR-34b/c together with miR-449 miRNAs as conserved regulators of multiciliogenesis [7,8,10-23].

In this study, we investigated the hypothesis of a second 'multiciliary locus' corresponding to the genomic locus around *MIR34B/C*. In humans, *MIR34B/C* genes are located near *C11orf88*, *LAYN*, and *BTG4*. *C11orf88*, of unknown function, has not yet been characterized in humans while *4833427G06Rik*, its murine ortholog, has been recently designated as *Hoatz* due to the Hydrocephalus and Oligo-Astheno-Terato-Zoospermia phenotype of *Hoatz* knockout mice [24]. HOATZ is required in flagellar and motile ciliogenesis notably by mediating the maturation of the flagellar glycolytic enzyme ENO4, though HOATZ may be involved in ciliogenesis with additional undetermined mechanisms [24]. *LAYN* gene codes for Layilin protein that has been described as a receptor of hyaluronan [25]. Finally, B cell translocation gene 4 (BTG4) belongs to the BTG/Tob protein family that controls transcription and mRNA turnover [26]. Although the BTG/Tob gene family has been examined in differentiation processes in other cellular contexts [26], the expression of *BTG4* during MCC differentiation remains still unexplored. In the present study, our findings provide evidence that (a) transcripts of *BTG4*, *LAYN*, and *HOATZ*, three proximal genes of the *MIR34B/C* locus, are expressed in both precursors and mature MCCs from human, mouse and pig models, (b) HOATZ protein is specifically and highly expressed in MCCs from the bottom to the tip of motile cilia, (c) LAYN proteins are expressed in both multiciliated and non-multiciliated cells and (4) *LAYN* silencing alters apical actin cap formation and multiciliogenesis.

Methods

Animals

All experiments were performed following the Directive 2010/63/EU of the European Parliament and of the council of 22 September 2010 on the protection of animals used for scientific purposes.

Mouse tracheal epithelial cell cultures

Each trachea was dissected from 12 weeks-old C57BL/6 mice (Charles River Laboratories, Wilmington, MA, USA) and placed in cold DMEM : F12 medium (1 : 1) supplemented with 15 mM HEPES, 100 U·mL^{-1} penicillin, 100 μg·mL^{-1} streptomycin, 50 μg·mL^{-1} gentamycin sulfate, and 2.5 μg·mL^{-1} amphotericin B. Each trachea was cleared under a binocular microscope to remove as much conjunctive tissue as possible and was opened longitudinally. Tracheas were then immersed overnight at 4 °C in supplemented DMEM : F12 containing 0.15% protease XIV from *Streptomyces griseus*. After incubation, tubes with the tracheas were agitated by inverting five times and let 10 min to reach room temperature. Tubes were reversed 10 times, FBS was added to a final concentration of 10%, and tubes were reversed again 20 times. Tracheas were transferred in a tube with supplemented DMEM-F12 containing 10% FBS, inverted 20 times, and the operation was repeated one more time in another tube. After discarding the tracheas, all the cell suspensions in the separate tubes were pooled and centrifuged at 500 *g* for 10 min at 4 °C. The pellet was resuspended in supplemented DMEM : F12 with 10% FBS and the cells were plated on regular cell culture plates and incubated in a humidified atmosphere of 5% CO$_2$ at 37 °C for 4 h to allow attachment of putative contaminating fibroblast. Cells in suspension were collected and centrifuged at 400 *g* for 5 min and were resuspended in DMEM-F12 containing BEGM Singlequot™ kit supplements (Lonza, Basel, Switzerland) and 5% FBS. Cells were then plated apically on rat-tail collagen I-coated Transwells® with medium in the basal side at ~ 30 000 cells per Transwell®. Medium was changed 48 h after, and every other day until confluency. Confluency was detected through the measure of the transepithelial electrical resistance (with EVOM2; World Precision Instruments, Sarasota, FL, USA). Once the resistance had reached a minimum of 1000 ohms·cm^{-2}, the apical medium was removed, and the basal medium was changed by Pneumacult-ALI™ medium (STEMCELL Technologies, Vancouver, Canada) to create ALI culture. This day corresponded to the differentiating step at day 0 (ALI0). Medium was then changed every other day. We analyzed mTEC differentiation at several time points (which were different from HNECs) including ALI0, ALI2, ALI3, ALI5, ALI6, ALI7, ALI9, ALI14 or ALI27, as indicated in figures and legends.

Mouse ependymal cell cultures

For the mouse ependymal cell cultures, experiments were performed using mouse Centrin-2-GFP-tagged ependymal cells as previously described [27]. Briefly, P0–P2 mice were sacrificed by decapitation. Brains were dissected in Hank's solution (10% HBSS, 5% HEPES, 5% sodium bicarbonate, 100 U·mL^{-1} penicillin, 100 µg·mL^{-1} streptomycin), and the telencephalon was manually cut into pieces, followed by enzymatic digestion (DMEM GlutaMAX, 3% papain (Worthington Biochemical, Lakewood, NJ, USA), 1.5% 10 mg·mL^{-1} DNAse, and 2.4% 12 mg·mL^{-1} cystein) for 45 min at 37 °C in a humidified 5% CO$_2$ incubator. The digestion was stopped by the addition of a solution of trypsin inhibitors (Leibovitz's L15 medium, 10% 1 mg·mL^{-1} ovomucoid, and 2% 10 mg·mL^{-1} DNAse). The cells were then washed in L15 medium and resuspended in DMEM GlutaMAX supplemented with 10% FBS and 1% penicillin/streptomycin in a poly-ʟ-lysine-coated flask. The ependymal progenitors were allowed to proliferate for 4–5 days, until confluence was reached, before being incubated overnight under shaking (250 r.p.m.). Cells were grown on 12-mm glass coverslips and were fixed on differentiation day 5.

Human samples

Inferior nasal turbinates were collected from patients with nasal obstruction (surgical intervention performed by L. Castillo at the Nice University Hospital, France) in Ca^{2+}/Mg^{2+}-free HBSS supplemented with 25 mᴍ HEPES, 200 U·mL^{-1} penicillin, 200 µg streptomycin, 50 µg·mL^{-1} gentamicin sulfate, and 2.5 µg·mL^{-1} amphotericin B (all reagent from Gibco/Thermo Fisher Scientific, Waltham, MA, USA). Human bronchial tissue samples were collected from healthy adult volunteers during bronchoscopy under local anesthesia. All procedures were administered by the same pulmonologist at Nice University Hospital, France. The process, location, and type of specimens (brushing or biopsy) were compatible with future use in daily clinical practice. These procedures have been performed according to the guidelines of the Declaration of Helsinki, after approval by the institutional review board 'Comité de Protection des Personnes Sud Méditerranée V' (06/06/2015, approval number: 17/081). The use of human tissues was authorized by bioethics law 94-654 of the French Public Health Code after written consent from the patients.

Human nasal epithelial cell cultures

Nasal turbinates were washed three times with cold-supplemented HBSS (Hepes 25 mᴍ, 200 U·mL^{-1} penicillin, 200 µg·mL^{-1} streptomycin, 2.5 µg·mL^{-1} amphotericin B, 50 µg·mL^{-1} gentamycin sulfate) and immersed in

supplemented HBSS containing 0.1% protease XIV from *S. griseus* (Sigma-Aldrich, Saint-Louis, MO, USA) overnight at 4 °C for epithelial digestion. Gentle agitation allowed to collect detached cells in inactivation buffer (DMEM supplemented with 10% FBS, 100 U·mL^{-1} penicillin, 100 µg·mL^{-1} streptomycin, 50 µg·mL^{-1} gentamicin sulfate, and 2.5 µg·mL^{-1} amphotericin B). After centrifugation at 150 *g* for 5 min, cells were resuspended in supplemented DMEM, centrifuged again, and then resuspended in bronchial epithelium basal medium (BEBM; Lonza) supplemented with BEGM SingleQuot™ Kit supplements (Lonza). Cell suspension was passed through a 21G needle, then plated (~ 20 000 cells·cm^{-2}) on 75 cm^2-flasks coated with rat-tail collagen I (Sigma-Aldrich), in and incubated in a humidified atmosphere of 5% CO$_2$ at 37 °C. After 24 h, cells were rinsed with PBS to remove erythrocytes and debris from the culture and immerged again in BEGM medium. After 4–5 days of culture, cells reached 70% confluence. They were detached using trypsin–EDTA 0.05% (Gibco) for 5–10 min, collected in inactivation buffer, centrifuged at 150 *g* for 5 min, and resuspended in BEGM medium. Cells were seeded on human placenta collagen IV-coated Transwell® permeable supports (6.5 mm diameter; 0.4 µm pore size; Corning, Corning, NY, USA) in the apical part with a density of ~ 30 000 cells per Transwell® and with medium in the basal part. Once the cells have reached confluence (~ 5 days after seeding), the medium was removed from the apical side of the Transwell® and the basal medium, replaced by Pneumacult-ALI™ (STEMCELL Technologies) to create ALI cultures as previously described [3,8,9]. This day corresponded to the differentiating step at day 0 (ALI0). Culture medium was changed every other day. We analyzed HNEC differentiation at several time points including ALI0, ALI6, ALI7, ALI10, ALI14, ALI15, ALI20, ALI22, and ALI28, as indicated in corresponding figures and legends. ALI day 0 (ALI0) is the time point at which cell cultures are switched to ALI in both HNECs and mTECs. Solitary primary cilia are detected in early ALI cultures usually from ALI0 to ALI12 before resorbing [28,29]. Then, a step of massive centriole amplification typically occurs around ALI1-ALI10 or ALI7-ALI14 in mTEC and HNEC cultures, respectively [3,9,29]. Then, the first motile cilia appear around ALI2-ALI7 or ALI15 in mTECs and HNECs or HBECs, respectively [3,8,9,28,29,30]. Fully-differentiated MCCs are detected around ALI5-ALI14 and ALI21-ALI28 for mTECs and HNECs or HBECs, respectively [3,7,8,9,28,29,30].

Human bronchial epithelial cell cultures

ALI HBECs were purchased from Epithelix® Sarl (Geneva, Switzerland) and cultured at ALI following the manufacturer's instructions.

Tissue processing for embedding

Human bronchial tissue biopsies were fixed in paraformaldehyde 4% (15 min at room temperature) and then extensively rinsed with PBS. Fixed tissues were then prepared for paraffin embedding. Cutting of paraffin-embedded sections was performed using a rotary microtome MICROM HM 340E (Thermo Fisher Scientific). Before staining, deparaffinization and antigen retrieval process were carried out on bronchial sections using citrate buffer at pH6. Sections and cytospins were permeabilized with 0.5% Triton X-100 in PBS. A following blocking treatment was performed with 3% bovine serum albumin (BSA) in PBS for 30 min. The incubation with primary antibodies was carried out at 4 °C overnight. Incubation with secondary antibodies was carried out during 1 h at room temperature. Nuclei were stained with 4,6-diamidino-2-phenylindole (DAPI).

Cytospins from human airway epithelial cell cultures

Cells dissociated from differentiated human nasal and bronchial epithelium cultured in ALI were cytocentrifuged at 72 *g* (800 r.p.m.) for 10 min onto SuperFrost™ Plus slides using a Shandon Cytospin™ 4 cytocentrifuge. Cytospin™ slides were fixed for 10 min in 4% paraformaldehyde at room temperature for further immunostaining.

Single-cell RNA-sequencing of HNECs, mTECs, and pig samples

Data used in the present study were generated from our previous study [3].

Cell dissociation of HNECs and mTECs

To perform single-cell analysis, cells on Transwells® at different days of ALI culture were incubated with 0.1% protease type XIV *S. griseus* (Sigma-Aldrich) in HBSS for 4 h at 4 °C. Then, cells were gently detached from the Transwell® by pipetting and transferred in a microtube. Cells were incubated at room temperature for 10 min with 50 units of DNase I (EN0523; Thermo Fisher Scientific) per 250 µL directly added in the tube. Cells were centrifuged at 150 *g* for 5 min and resuspended in 500 µL of supplemented HBSS containing 10% FBS, centrifuged again at 150 *g* for 5 min, and resuspended in 500 µL HBSS with 10% FBS and dissociated mechanically four times through a 26-G syringe. Finally, cell suspensions were filtered through a 40-µm porosity Flowmi™ Cell Strainer (Bel-Art, Wayne, NJ, USA), centrifuged at 150 *g* for 5 min, and resuspended in 500 µL of HBSS. Cell concentration was measured with Scepter™ 2.0 Cell Counter (Merck Millipore, Darmstadt, Germany) and Countess™ automated cell counter (Thermo Fisher Scientific). Cell viability was checked with Countess™ automated

cell counter (Thermo Fisher Scientific). All steps except the DNase I incubation were performed on ice. Cell concentration was adjusted to 300 cells·µL^{-1} in HBSS for the cell capture by 10× Genomics device, in order to capture 1500 cells for HNECs and 5000 cells for mTECs.

Single-cell isolation and library construction

We followed the manufacturer's protocol (Chromium™ Single-Cell 3′ Reagent Kit, v2 Chemistry, 10X Genomics, Pleasanton, CA, USA) to obtain single-cell 3′ libraries for Illumina sequencing. Libraries were sequenced with a NextSeq 500/550 High Output v2 kit (75 cycles) (Illumina, San Diego, CA, USA) that allows up to 91 cycles of paired-end sequencing: Read 1 had a length of 26 bases that included the cell barcode and the unique molecular identifier (UMI); Read 2 had a length of 57 bases that contained the cDNA insert; Index reads for sample index of 8 bases.

Single-cell RNA-seq data analysis

CELL RANGER SINGLE-CELL Software Suite v1.3 (10X Genomics) was used to perform sample demultiplexing, barcode processing, and single-cell 3′ gene counting using standards default parameters and human build hg 38, pig build sus scrofa 11.1 and mouse build mm10. Individual dataset analysis was performed using SEURAT standard analysis pipeline [31]. Briefly, cells were first filtered based on the number of expressed features, dropout percentage, library size, and mitochondrial gene percentage. Thresholds were selected by visually inspecting violin plots in order to remove the most extreme outliers. Genes expressing less than 5 UMI across all cells were removed from further analysis. Cell-level normalization was performed using the median UMI counts as a scaling factor. Highly variable genes (hvgs) were selected for the following analysis based on their expression level and variance. PCA analysis was performed on those hvgs, and the number of PCs to use was chosen upon visual inspection of the PC variance elbow plot (~ 10–20 PCs depending on the dataset). Clustering was first performed with the default parameter and then increasing the resolution parameter above 0.5 to identify small clusters (but with the knowledgeable risk of splitting big cluster due to high gene expression variability). Differential analysis was again performed using SEURAT FindAllMarkers and FindMarkers functions based on the nonparametric Wilcoxon rank-sum test. All graphs were generated using SEURAT and GGPLOT2 [32] in the free software environment R (http://www.r-project.org).

RNA interference

Before seeding (60 000 cells per Transwell®) HNECs were transfected with a mixture of four individual siRNAs against human *LAYN* transcript or siRNAs scrambled

(5 nM final concentration) (ON-Target plus SMARTpool; Dharmacon Horizon Discovery, Lafayette, CO, USA) using Lipofectamine RNAi Max Reagent (Invitrogen) in OPTIMEM (Invitrogen/Thermo Fisher Scientific) according to the manufacturer's instructions. The cells were then harvested as in normal conditions.

Immunostainings

Human and mouse airway epithelial samples were fixed with 4% paraformaldehyde (20 min, 4 °C), washed in PBS, permeabilized with 0.5% Triton X-100 (5 min, room temperature), and blocked with 3% BSA in PBS (30 min, room temperature). Incubation with primary antibodies was carried out at 4 °C overnight, as follows: rabbit polyclonal anti-LAYN (1 : 200, HPA-040087; Sigma-Aldrich), goat polyclonal anti-HOATZ (C11orf88) (1 : 100, SC-270467; Santa Cruz Biotechnology, Dallas, TX, USA), rabbit polyclonal anti-C11orf88-DNAxPab (HOATZ) (1 : 100, H00399949-W01P; Abnova, Taipei City, Taiwan), mouse monoclonal antiacetylated alpha-tubulin (1 : 1000, Clone 6-11B-1; Sigma-Aldrich), rabbit polyclonal anti-SNTN (sentan) (1/50, ab122845; Abcam, Cambridge, UK), mouse monoclonal anticentrin-2 (1 : 200, clone (N-17)-R; Santa Cruz Biotechnology). Incubation with secondary antibodies (1 : 500, Alexa Fluor; Thermo Fisher Scientific) was carried out for 1 h at room temperature and protected from light. Transwell® membranes were cut with a razor blade and mounted on slides with Fluoromount-G™ mounting medium with DAPI (Thermo Fisher Scientific).

Mouse ependymal cells were fixed for 10 min in either 4% paraformaldehyde at room temperature or 100% ice-cold methanol at −20 °C. Cells were preblocked in PBS with 0.2% Triton X-100 and 10% FBS before incubation with the primary and secondary antibodies. Centrin-2-GFP-tagged ependymal cells were co-stained with mouse anti-GT335 to detect cilia (1 : 500, AG-20B-0020-C100; Adipogen, San Diego, CA, USA) and with goat polyclonal anti-HOATZ (C11orf88) (1 : 100, SC-270467; Santa Cruz Biotechnology), followed by an incubation with species-specific Alexa Fluor secondary antibodies (1 : 400; Life Technologies/Thermo Fisher Scientific). Cells were counterstained with DAPI (10 μg·mL^{-1}; Sigma-Aldrich) and mounted in Fluoromount (Thermo Fisher Scientific).

Images were acquired using the Olympus Fv10i (Olympus, Tokyo, Japan) or Leica SP5 or Leica SP8 (Leica Microsystems, Nanterre, France) confocal imaging systems.

Confocal and stimulated emission depletion microscopy

Samples were mounted either in Fluoromount-G mounting medium with DAPI (for confocal) or in Abberior Mount Solid Antifade (Abberior GmbH, Göttingen, Germany) (for STED). Images were acquired using a Leica SP8 STED 3× (Leica Microsystems), at 700 Hz either through a 63×/1.4 NA Oil objective (for confocal) or through a 93×/1.3 NA Glyc objective (for STED), using the LAS X software (Leica Microsystems). Confocal images were obtained by a 405-, 488-, and 561-nm laser excitation, respectively. All images have a 72-nm pixel size Super-resolution images were obtained using STED microscopy with 561 and 633-nm excitations and the depletion at 775 nm for both fluorophores (20–30% of power). Images obtained in STED had a 17-nm pixel size. The images were deconvolved using HUYGENS PROFESSIONAL (version 18.10; Scientific Volume Imaging, Hilversum, The Netherlands, http://svi.nl), using the CMLE algorithm with SNR:20 and 40 iterations (for confocal) or with SNR:100 and 5 iterations (for STED).

Western blot experiments

Cells were collected by scrapping in antiprotease supplemented Ripa lysis Buffer (Pierce/Thermo Fisher Scientific), ultrasonicated, and cleared by centrifugation. Protein concentration was determined using the BCA assay (Thermo Fisher Scientific), and 25 μg of protein was resolved on SDS polyacrylamide gels using gradient Bolt SDS/PAGE Gel System following the manufacturer's instructions. Proteins were transferred to PVDF membranes; membranes were blocked with 5% milk in TBS-Tween buffer for 1 h. Incubation with primary antibodies (mouse monoclonal anti-LAYN 1 : 500, Santa Cruz, sc377389; goat polyclonal anti-HOATZ 1 : 100, Santa Cruz Biotechnology, SC-270467; rabbit polyclonal anti-HOATZ-DNAxPab 1 : 100, H00399949-W01P, Abnova; mouse monoclonal anti-GAPDH 1 : 20 000, 60004-1, ProteinTech, San Diego, CA, USA; and goat polyclonal anti-HSP60 1 : 5000, sc-1052, Santa Cruz Biotechnology, Inc), in 5% milk in TBS-Tween buffer, was carried out at 4 °C overnight. After three washes with TBS-Tween buffer during 10 min at room temperature, membranes were incubated with HRP-conjugated secondary antibodies (diluted at the required concentration) at room temperature for 1 h. After three washes, immunoreactive bands were detected using immobilon ECL kit (Merck Millipore) on Fusion-FX imager (Vilber, Marne-La-Vallée, France).

Results

Transcript expression of the *MIR34B/C* gene members during airway epithelium regeneration

In order to identify cell type-specific expression of *HOATZ* (*C11orf88*), *LAYN*, and *BTG4*, three proximal genes of the conserved *MIR34B/C* genomic locus (Fig. 1A), we have used single-cell RNA-seq (scRNA-seq) *in vitro*, on both human nasal epithelial cells (HNECs) and mouse tracheal epithelial cells (mTECs) differentiated at the air-liquid interface (ALI), and *in vivo*, in human airway biopsies and
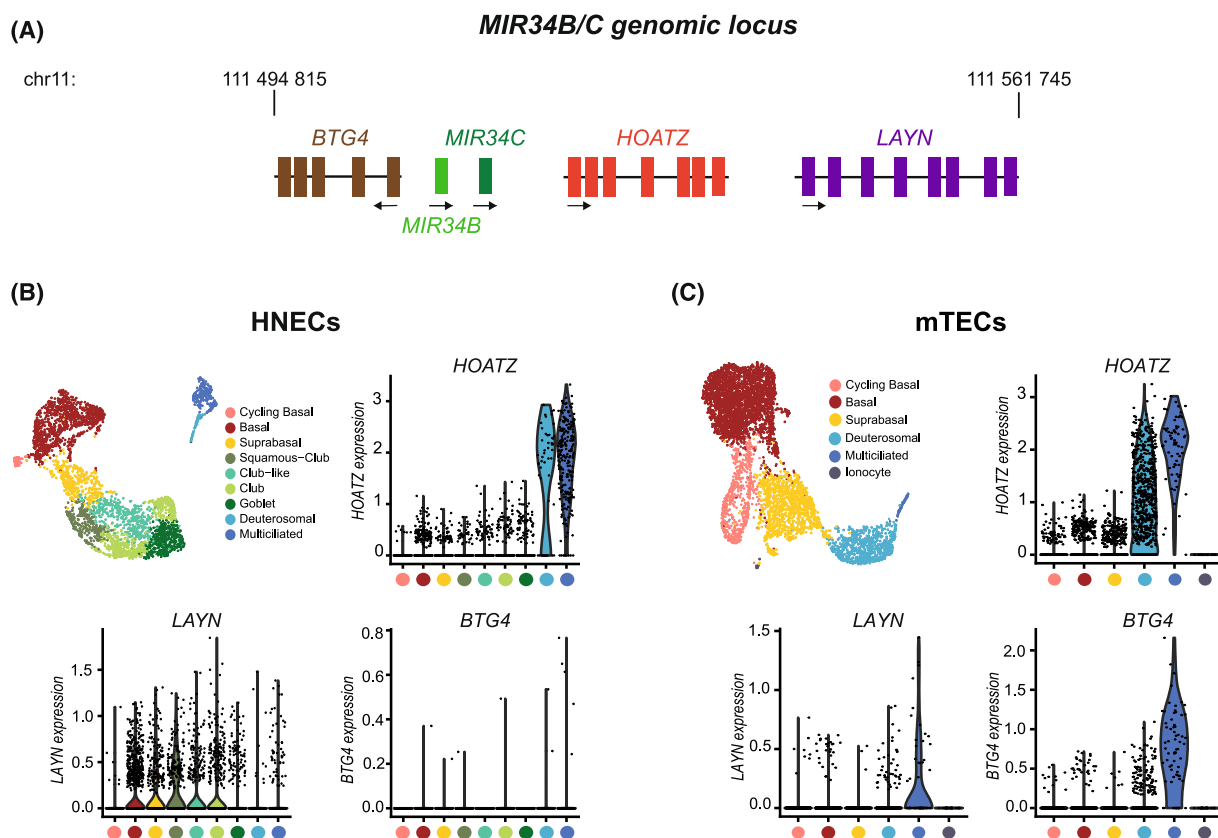
Fig. 1. Expression and localization of the *MIR34B/C* locus members in multiciliated epithelia from human and mouse. (A) Illustration of the positioning of three proximal genes around the *MIR34B/C* genomic locus. Exon lengths and positions are not strictly proportional to actual annotations. Genomic start and end positions of the locus are accurate and indicated on the top. (B) Transcript expression of the *MIR34B/C* locus members is enriched in MCCs of the human airway epithelium: UMAP (top left panel) illustrating single-cell RNA-sequencing data from fully-differentiated HNECs in Pneumacult-ALI™ medium (ALI28) clustered 9-cell populations. Violin plots (top right and bottom panels) representing the level of normalized gene expression in each cell population for *HOATZ*, *LAYN*, and *BTG4*. (C) Transcript expression of the *MIR34B/C* locus members is enriched in MCCs of the murine tracheal epithelium: UMAP (top left panel) illustrating single-cell RNA-sequencing data obtained with mouse tracheal epithelial cells (mTECs) at mid-differentiation (ALI3). Violin plots (top right and bottom panels) representing the level of normalized gene expression in each cell population for *HOATZ*, *LAYN*, and *BTG4*.

brushings [2], as well as in newborn pig airways. All scRNA-seq datasets showed that *HOATZ* transcripts were specifically and strongly expressed in both mature MCCs and their precursors (deuterosomal cells) in all models: human (Fig. 1B; Fig. S1A for *in vitro* data; Fig. S2A,B for *in vivo* data), mouse (Fig. 1C; Fig. S1B) or pig (Fig. S3A, B,E,F). Two isoforms of human *HOATZ* transcripts were described in Ensembl Genome Browser: *HOATZ-201* (ENST00000332814) with 7 exons and *HOATZ-202* (ENST00000375618) with 6 exons (Fig. S4A). Using long-read RNA-sequencing and RT-PCR, our data showed that both *HOATZ* transcript isoforms were expressed in differentiated HNECs (Fig. S4A,B), with an overrepresentation of *HOATZ-202* compared with *HOATZ-201* (Fig. S4A).

LAYN expression was also specific to MCCs in mice and pigs but was more ubiquitous in human with

detection in all cell types (Fig. 1B,C; Figs S2C and S3C,G).

BTG4 was expressed in a few cells in humans and pigs, most of them being MCCs, both *in vitro* and *in vivo* (Fig. 1B,C; Figs S2D and S3D,H). Fortuitously, we found out that *BTG3*, another gene belonging to the BTG/Tob family, for which the level of expression and the number of *BTG3*-expressing cells were much higher than the one of *BTG4* in human cells, was markedly expressed in human deuterosomal cells and also moderately expressed in mature MCCs (Fig. S5).

When analyzing transcript expression in a time-course manner, by RNA-seq and RT-qPCR, the expression of *HOATZ* and *BTG4* increased concomitantly to *FOXJ1* (a marker of MCCs) and *CDC20B* (a

marker of deuterosomal cells) in both HNECs and mTECs (Fig. S1C–F) [9,33]. In agreement with the scRNA-seq data, *Layn* expression was increased during multiciliogenesis of mTECs and remained constant in HNECs (Fig. S1C–F).

HOATZ proteins are localized in motile cilia in human and mouse MCCs

HOATZ protein subcellular localization was assessed from ALI cultures (HNECs, human bronchial epithelial cells (HBECs) or mTECs), native human bronchial tissue (biopsy sections), and mouse ependymal cells by immunostaining followed by confocal or stimulated emission depletion (STED) microscopy. Antibodies against HOATZ were validated by western blot (Fig. S4C,D). In early ALI cultures, HOATZ was first detected in a punctate manner in the primary cilium of mTECs, while it was not detected in the primary cilium of HNECs (Fig. 2A). At early steps of the formation of motile cilia, when cilia have not fully elongated, HOATZ was mainly detected at the tip of cilia (Fig. 2B,C) and partially co-localized with Sentan (SNTN) (Fig. 2C), the first described molecular component of the ciliary tip of vertebrate motile cilia [34]. This was well observed using confocal and super-resolution STED microscopy at 12–14 days of differentiation for HNECs (Fig. 2B,C), 2 days for mTECs (Fig. 3A) and 5 days for ependymal cells (Fig. 3B). Later in differentiation, mature MCCs displayed longer motile cilia in which HOATZ was highly detected from the bottom of cilia until the ciliary tip, with a punctate pattern in all models, including on ALI cultures or cytospin-isolated HNECs and HBECs (Fig. 2B,D,E), as well as on native human bronchial tissue sections (Fig. 2F) and mouse ependymal cells (Fig. 3B).

Localization of LAYN proteins in both human and mouse models of airway epithelium

As shown by immunostaining, LAYN protein was absent from the primary cilium in mTECs but appeared as a punctate distribution along the motile cilia in mid- and fully-differentiated MCCs (Fig. 4A). A distinct pattern of expression was observed in HNECs, where LAYN expression was not restricted to MCCs and was detected in the cytoplasmic region with an apical polarization in fully-differentiated MCCs (Fig. 4B). An apical surface localization of LAYN has already been reported in human airway epithelial cells [25]. In HNECs, LAYN was also expressed in other cells than MCCs, which is consistent with our scRNA-seq data (Fig. 1B; Fig. S2C). The distinct expression and localization of LAYN in mouse and human airway epithelium may refer to distinct roles in the two species. To assess the role of LAYN in HNEC differentiation, we performed siRNA silencing using siRNAs against human *LAYN* transcripts 4 days before ALI differentiation. Expression analysis from ALI0 to ALI14 showed that siRNAs efficiently knocked-down LAYN both at the RNA and protein levels (Fig. S6A–C) and that *LAYN* RNA levels started to reverse back to control level from day 7 (Fig. S6A). Upon differentiation, the level of *FOXJ1* transcripts (ALI14, Fig. S6C) and the proportion of centrin-2-positive (ALI20, Fig. 4C,D) or acetylated alpha-tubulin-positive MCCs (ALI20, Fig. 4E,F) were significantly lower in cultures transfected with siRNAs against *LAYN* transcripts compared with control. In addition, the apical actin meshwork was strongly altered in si*LAYN* conditions (Fig. 4G), revealed by a reduction of the enrichment of the phalloidin-stained apical actin cap and a decrease in the number of cells exhibiting an enrichment of apical actin meshwork corresponding to MCCs. These observations also suggest defects in polarization and basal body anchoring. Therefore, inhibition of *LAYN* expression at an early stage of differentiation appears sufficient to alter the subsequent formation of MCCs.

Discussion

This work represents the first characterization of the expression of three genes belonging to the *MIR34B/C* genomic locus. The first observation is that *HOATZ* expression was strikingly increased in both deuterosomal and MCCs during human, mouse, or pig airway epithelium regeneration. It is noteworthy that *HOATZ* expression was maintained in MCCs, while gene expression from the *MIR449* genomic locus rapidly decreased after the deuterosomal stage. The punctate pattern of HOATZ proteins in the primary cilium of mTECs is probably related to a functional role played in the primary cilium before multiciliogenesis. Indeed, cells with a primary cilium acquire markers of motile ciliogenesis and MCCs may originate from primary ciliated cells as previously described elsewhere [28]. The ciliary tip, at the distal end of the cilium, is a putative site of axonemal growth and resorption and may be involved in the regulation of the intraflagellar transport (IFT) [35]. Using super-resolution microscopy, we showed that HOATZ was partially co-localized with SNTN in the ciliary tip region, suggesting a role of HOATZ either in the assembly of the microtubule doublets during the elongation of axoneme, in the
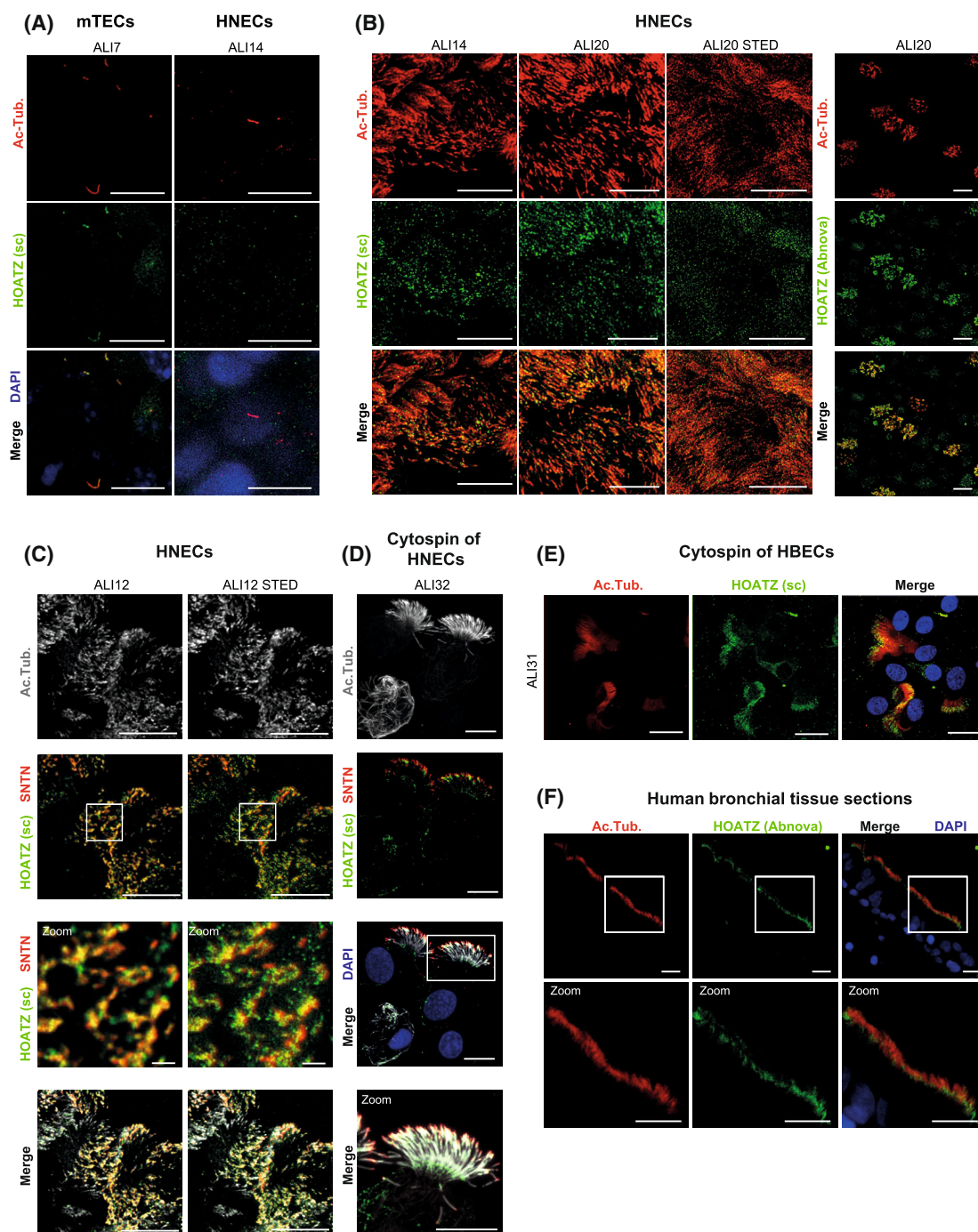
Fig. 2. Expression of HOATZ in primary and motile cilia in mouse and human airway cells. (A) Immunostainings performed on mTECs at ALI7 or in HNECs at ALI14, for acetylated alpha-tubulin (Ac. Tub.) and HOATZ. Regions of the cell culture devoid of MCCs were selected to show immunostaining of solitary primary cilium. (B) Immunostainings carried out on HNECs at ALI14 and ALI20 for acetylated alpha-tubulin (Ac. Tub.) and HOATZ. (C) Immunostainings carried out on HNEC cultures (ALI12) for HOATZ, SNTN, and acetylated alpha-tubulin (Ac. Tub.). (D) Immunostainings performed on cytospin-isolated HNECs (ALI32) for HOATZ, SNTN, and acetylated alpha-tubulin (Ac. Tub.). (E) Immunostainings performed on cytospin-isolated HBECs (ALI31) for HOATZ and acetylated alpha-tubulin (Ac. Tub.). (F) Immunostainings performed on human bronchial tissue sections for HOATZ and acetylated alpha-tubulin (Ac. Tub.). Scale bars for all images: 10 μm, except for zoom images in (C), scale bars: 1 μm. sc: Santra Cruz sc-270467 antibody; Abnova: DNAxPab, H00399949 antibody. Images were obtained by confocal microscopy or, when indicated, by super-resolution STED microscopy.
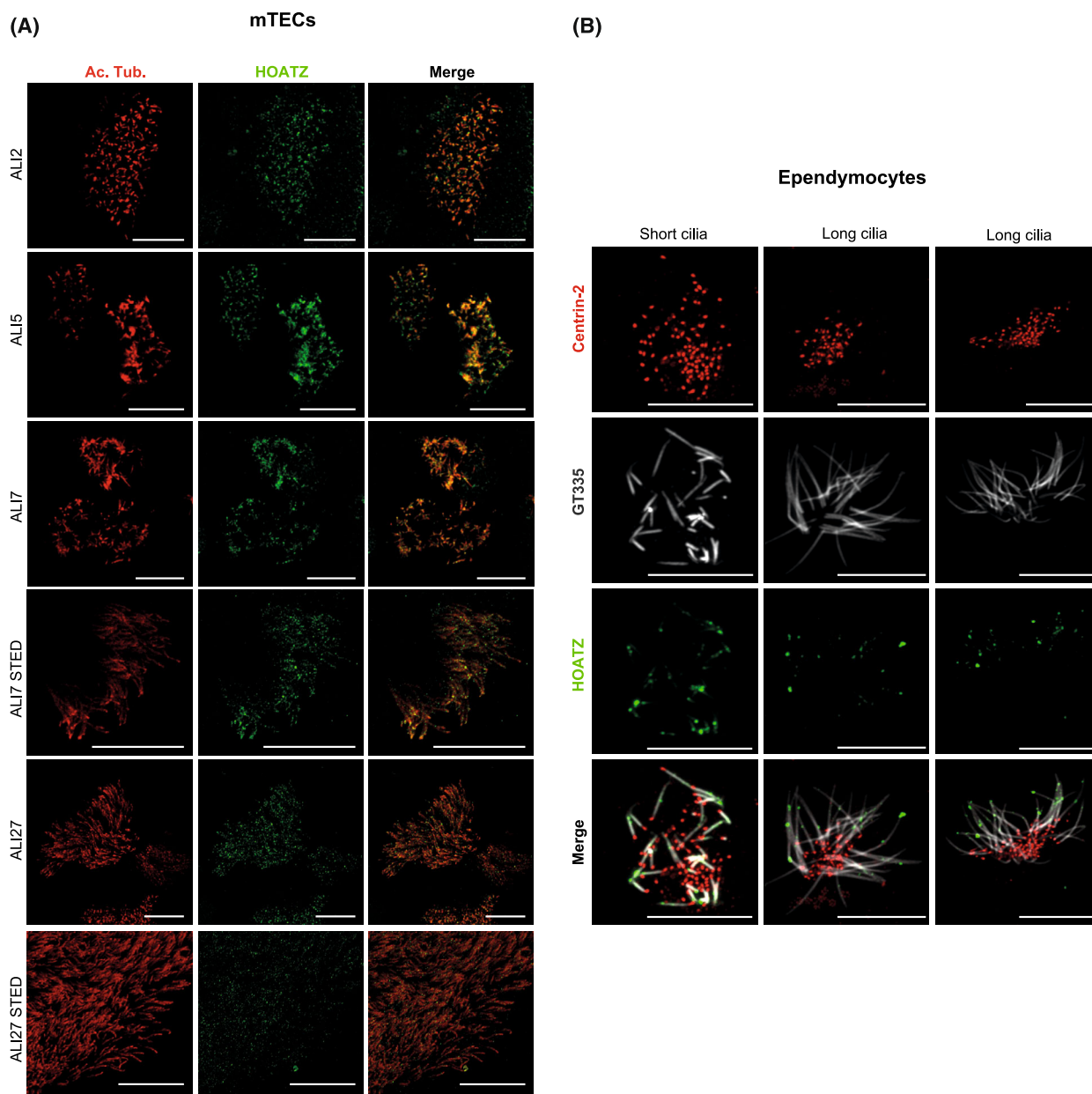
Fig. 3. Expression of HOATZ in motile cilia throughout the differentiation of mouse tracheal epithelial cells (mTECs) and in mouse ependymal cells. (A) Immunostainings performed on mTECs at ALI2, ALI5, ALI7, and ALI27 for HOATZ and acetylated alpha-tubulin (Ac. Tub.). (B) Immunostainings performed on mouse ependymal cells expressing Centrin-2-GFP (shown in red) at day 5 of differentiation, with antibodies against GT335, a marker of cilia glutamylation, and against HOATZ. The first line of panels illustrates maturing MCCs exhibiting shorter cilia. The second and third lines of panels illustrate mature MCCs with longer cilia. Scale bars for all images: 10 μm. Images were obtained by confocal microscopy or, when indicated, by super-resolution STED microscopy.

control of the ciliary length or in the formation of the ciliary cap at the tip. Moreover, the punctate pattern of HOATZ in motile cilia may evoke a role in the transport of components during the building and maintenance of cilia. HOATZ may be a component of trains, or cargo of this transport, or may be carried by IFT along the cilia to play a role in the axoneme. A recent study in mice showed that *Hoatz* was required for motile ciliogenesis in ependymal cells and sperm flagella genesis by mediating the maturation of the flagellar glycolytic enzyme enolase-4 ENO4. Indeed, ENO4, which is specifically expressed in ciliated cells, is actively transported along the motile cilia in mice, suggesting the importance of glycolytic enzymes in
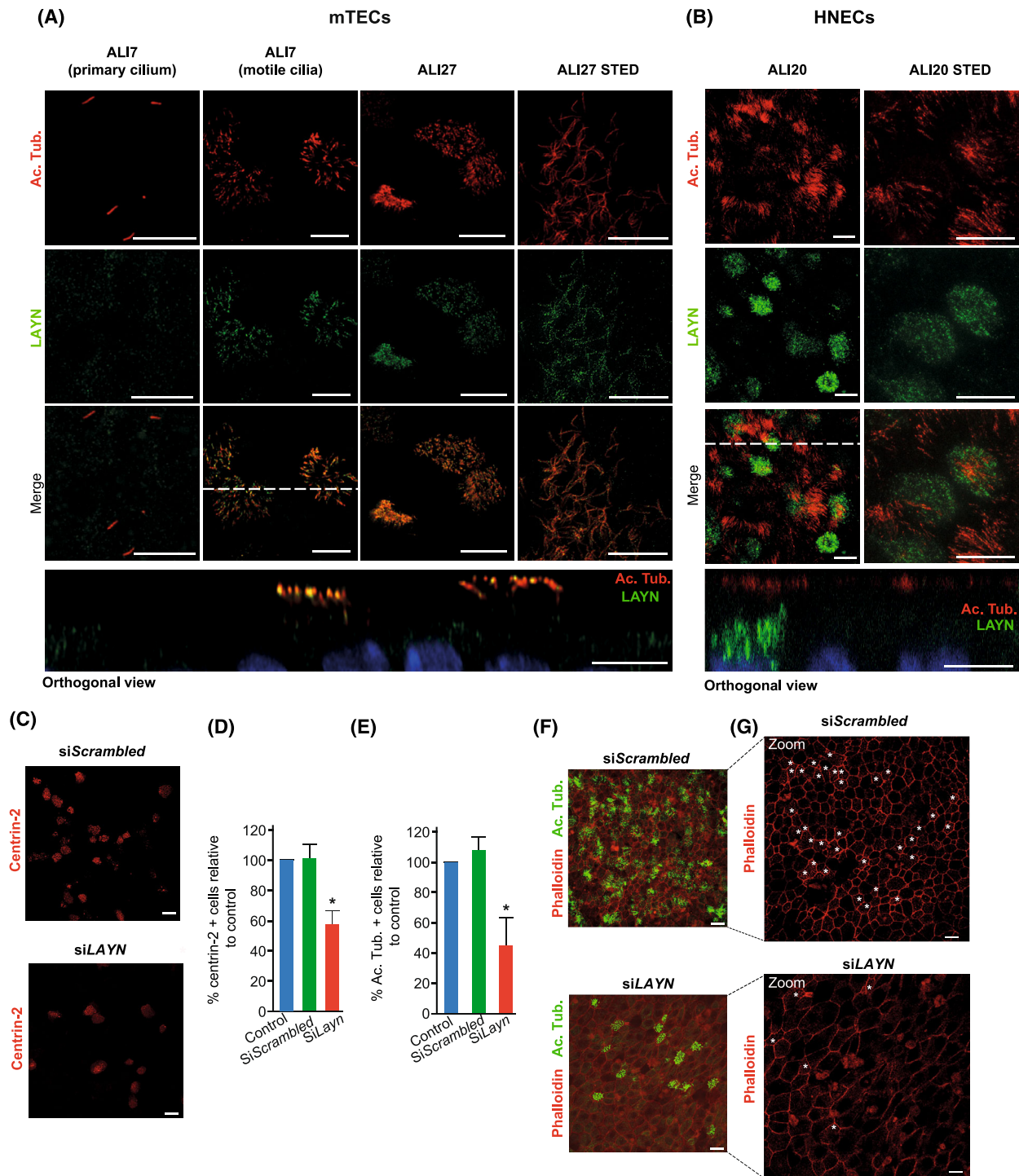
local ATP production in highly energy-demanding cell types such as MCCs [24]. In agreement with this, we also observed in our datasets that *ENO4* transcripts were mainly detected in deuterosomal and MCC populations: about 30% (in HNECs) and 37% (in mTECs)

of MCC/deuterosomal cells co-expressed *HOATZ and ENO4*. A small proportion of deuterosomal cells or MCCs (0.6% in HNECs and 4.6% in mTECs) expressed *ENO4* without *HOATZ* (Table S1). These observations corroborate the previous conclusions of

Fig. 4. LAYN expression and function during multiciliogenesis. (A) Immunostainings performed on mTECs at ALI7 and ALI27 for LAYN and acetylated alpha-tubulin (Ac. Tub.). (B) Immunostainings carried out on HNECs at ALI20 for LAYN and acetylated alpha-tubulin (Ac. Tub.). The bottom panel is an orthogonal view from the top image, performed at the level of dashed line. Scale bars: 10 μm. (C) Immunostainings performed on HNECs (ALI20) for centrin-2 after LAYN knock-down by siRNAs (si*LAYN*). (D) The bar plot indicates the percentage of centrin-2+ cells (over nuclei numbers), relative to the control set to 100%, and calculated from immunostainings on HNECs (ALI20) after LAYN knock-down by siRNAs (si*LAYN*). The control condition refers to nontransfected cells. siScrambled: transfection with scrambled siRNAs. Data are mean ± SD from 10 fields per insert, *n* = 3 independent experiments (*$P < 0.05$; Student's *t*-test). (E) The bar plot indicates the percentage of Ac. Tub. + cells (over nuclei numbers), relative to the control set to 100%, and calculated from immunostainings on HNECs (ALI20) after LAYN knock-down by siRNAs (siLAYN). The control condition refers to nontransfected cells. siScrambled: transfection with scrambled siRNAs. Data are mean ± SD from 10 fields per insert, *n* = 3 independent experiments (*$P < 0.05$; Student's *t*-test). (F) Immunostainings performed on HNECs (ALI20) for acetylated alpha-tubulin (Ac. Tub.) and actin network (Alexa Fluor™ Phalloidin-647) after LAYN knock-down by siRNAs (si*LAYN*). (G) Blow-up images from phalloidin staining in (F). White asterisks indicate in a nonexhaustive manner MCC with enriched apical actin cap in siScrambled compared withf si*LAYN* conditions, in representative images. Scale bars: 10 μm. Images were obtained by confocal microscopy or, when indicated, by super-resolution STED microscopy.

Narita *et al.* [24], which proposed that HOATZ was involved in the maturation of ENO4 and contributed to metabolic pathways for energy production in the cilia.

The second gene of the *MIR34B/C* locus that we investigated was *LAYN*. In humans, *LAYN* transcripts were expressed in deuterosomal cells and, to a lesser extent, in mature MCCs, but they were also detected in other cell types including basal, suprabasal, and secretory cells. We detected the Layilin protein as punctate spots along the motile cilia in mouse tracheal MCCs, whereas it was localized in a cytoplasmic region, with an apical polarization in human airway MCCs. An apical surface localization of LAYN in airway epithelial cells has already been reported in human airway epithelium in ALI cultures. This previous study has described that the signal of hyaluronan binding on LAYN acted through RhoA/ROCK pathway [25]. We showed that *LAYN* silencing at an early stage of differentiation was sufficient to alter the subsequent formation of MCCs with defects in apical actin network. This observation suggests that the early absence of LAYN may prevent some key events, which will be detrimental to the rest of MCC differentiation, such as polarization and actin network formation. So, it is possible that in si*LAYN* conditions, the MCC differentiation may be prevented because of these early stages that the cells did not go through. In these conditions, restoration of *LAYN* levels at ALI14 may not be sufficient to fully restore MCC differentiation. The dependence of multiciliogenesis on the actin cytoskeleton has been well documented by numerous studies including ours. The apical surface of MCCs is enriched with a dense meshwork of actin composed of two distinct parts, the apical and the subapical actin networks. This apical actin network is essential for both polarization and motility of the cilia. Defects in this apical actin network have been shown to impair

basal body transport, localization, polarity, docking, and stability [7,19,36,37,38]. Previously, we have reported that miR-34/449 controls apical actin network reorganization by modulating small GTPase pathways, including RhoA [7,19]. The localization of LAYN near the apical membrane in MCCs, combined with the alteration of the apical actin web and MCC formation in response to *LAYN* silencing and with the previously described interaction of LAYN with RhoA/ROCK signal [25] are consistent with a putative role played by *LAYN* in the remodeling of apical cytoskeleton that contributes to the basal body anchoring in MCCs. Hyaluronic acid is secreted by submucosal glands, but its function in airway secretions other than influencing the rheology of mucus is not fully understood. Since hyaluronic acid has already been shown to contribute to ciliary differentiation and beating in human airway epithelium [39,40], we can speculate that LAYN might also contribute to ciliary beating in fully-differentiated airway epithelium.

Finally, we provide some observations about *BTG4*, the third gene of the *MIR34B/C* locus. However, due to the weak BTG4 expression in our different models and the lack of available antibodies giving a specific signal for BTG4 in our models, a more descriptive study is limited at this time. We, however, noticed that MCCs express higher levels of *BTG4* compared with deuterosomal cells. In addition, a previous study indicated that BTG4 was highly expressed in ciliated epithelial tissues of juvenile mice such as pharynx, trachea, oviduct, and testis but expressed at lower levels in adult mice [41]. While human diseases caused by mutations in *BTG4* have not been clearly identified, some homozygous mutations in *BTG4* have been associated with zygotic cleavage failure and female infertility through a mechanism involving the maternal mRNA decay in mammalian oocytes [42]. Nevertheless, these authors did not examine the MCC

phenotype in the reproductive tract of women carrying *BTG4* mutations and diagnosed with infertility. BTG4 also prevents the progression of oocytes into anaphase II by ensuring that the anaphase-promoting complex/cyclosome (APC/C) is completely inhibited during the arrest [43]. Furthermore, PLK1 controls the onset of spindle assembly and formation and is essential for APC/C activation before anaphase onset in mouse zygotes [44]. This mechanism could be connected to our previous work showing that the *MIR449* gene member CDC20B cooperates around deuterosomes with PLK1 and APC/C activation to trigger centriole disengagement in maturing MCCs [9]. Moreover, the expression of *BTG3*, another gene belonging to the BTG/Tob family, was stronger than *BTG4* in both deuterosomal cells and MCCs. In another context, *BTG3* has been shown to inhibit BMP2 signaling during osteoblast differentiation [26], and we have previously shown that BMP2 signal inhibition strongly stimulated the formation of MCCs [30]. The role of the BTG/Tob family as negative regulators of the cell cycle [45] and the use of cell cycle actors for the amplification of centrioles in MCCs reported in our recent studies [3,9] may suggest a putative role of some members of the BTG/Tob family such as BTG4 or BTG3 in MCC differentiation.

In conclusion, our study demonstrates that the transcripts of *BTG4*, *LAYN*, and *HOATZ*, three proximal genes of the *MIR34B/C* locus, are expressed in human, mouse, and pig MCCs. Especially, we have described in different models, human and mouse, the precise site of HOATZ expression in motile cilia, its enrichment at the tip of the cilia, more particularly in developing epithelium, and its more punctiform profile from the bottom to the tip of motile cilia in fully-differentiated epithelium (Fig. S7). Using a knockout mouse model, HOATZ has been shown by others to be required for the motile cilia function of ependymal cells or sperm flagellum formation [24]. These data collectively argue that HOATZ represents a novel conserved motile ciliogenesis actor. We have also observed that early inhibition of *LAYN* expression dramatically impairs apical actin cap formation and MCC differentiation, probably through indirect mechanisms given the expression pattern of LAYN. Altogether, our data indicate that, as previously observed for *MIR449* genomic locus [8,9,10,46,47], the *MIR34B/C* locus also encompasses some genes that may be involved in MCC biology. Further investigations of loss or gain of function using approaches such as CRISPR-Cas9 in different models would be needed to elucidate the precise role of each of these genes in multiciliogenesis.

Data accessibility

Single-cell RNA-seq datasets used in the present study were generated from our previous studies [2,3]. All scRNA-seq data generated from our previous study [2] are currently available through the European Genome-

phenome Archive (EGAS00001004082), and sequence-free data will be linked to the Data Central Repository of the Human Cell Atlas, in order to ensure the openness of information. Data are also available through a dedicated web interface (https://www.genomique.eu/cellbrowser/HCA/). Datasets generated from our previous study [3] have been previously deposited in GEO under the series number GSE121600. Links to the UCSC cell browser for data visualization are genomique.info/cellbrowser/Differentiation/Pneumacult/ and genomique.info/cellbrowser/Differentiation/BEGM/. All other data are available from the authors.

References

1 Zaragosi LE, Deprez M and Barbry P (2020) Using single-cell RNA sequencing to unravel cell lineage relationships in the respiratory tract. *Biochem Soc Trans* **48**, 327–336.

2 Deprez M, Zaragosi LE, Truchi M, Becavin C, Ruiz García S, Arguel MJ, Plaisant M, Magnone V, Lebrigand K, Abelanet S *et al.* (2020) A single-cell atlas of the human healthy airways. *Am J Respir Crit Care Med* **202**, 1636–1645.

3 Ruiz Garcia S, Deprez M, Lebrigand K, Cavard A, Paquet A, Arguel M-J, Magnone V, Truchi M, Caballero I, Leroy S *et al.* (2019) Novel dynamics of human mucociliary differentiation revealed by single-cell RNA sequencing of nasal epithelial cultures. *Development* **146**, dev177428.

4 Legendre M, Zaragosi LE and Mitchison HM (2021) Motile cilia and airway disease. *Semin Cell Dev Biol* **110**, 19–33.

5 Spassky N and Meunier A (2017) The development and functions of multiciliated epithelia. *Nat Rev Mol Cell Biol* **18**, 423–436.

6 Zhao H, Zhu L, Zhu Y, Cao J, Li S, Huang Q, Xu T, Huang X, Yan X and Zhu X (2013) The Cep63 paralogue Deup1 enables massive de novo centriole biogenesis for vertebrate multiciliogenesis. *Nat Cell Biol* **15**, 1434–1444.

7 Chevalier B, Adamiok A, Mercey O, Revinski DR, Zaragosi L-E, Pasini A, Kodjabachian L, Barbry P and Marcet B (2015) miR-34/449 control apical actin network formation during multiciliogenesis through small GTPase pathways. *Nat Commun* **6**, 8386.

8 Marcet B, Chevalier B, Luxardi G, Coraux C, Zaragosi LE, Cibois M, Robbe-Sermesant K, Jolly T, Cardinaud B, Moreilhon C *et al.* (2011) Control of vertebrate multiciliogenesis by miR-449 through direct repression of the Delta/Notch pathway. *Nat Cell Biol* **13**, 693–699.

9 Revinski DR, Zaragosi L-E, Boutin C, Ruiz-Garcia S, Deprez M, Thomé V, Rosnet O, Gay A-S, Mercey O, Paquet A *et al.* (2018) CDC20B is required for

deuterosome-mediated centriole production in multiciliated cells. *Nat Commun* **9**, 4668.

10 Loukas I, Skamnelou M, Tsaridou S, Bournaka S, Grigoriadis S, Taraviras S, Lygerou Z and Arbi M (2021) Fine-tuning multiciliated cell differentiation at the post-transcriptional level: contribution of miR-34/449 family members. *Biol Rev Camb Philos Soc* **96**, 2321–2332.

11 Wu YJ, Liu Y, Hu YQ, Wang L, Bai FR, Xu C and Wu JW (2021) Control of multiciliogenesis by miR-34/449 in the male reproductive tract through enforcing cell cycle exit. *J Cell Sci* **134**, jcs253450.

12 Yuan S, Liu Y, Peng H, Tang C, Hennig GW, Wang Z, Wang L, Yu T, Klukovich R, Zhang Y *et al.* (2019) Motile cilia of the male reproductive system require miR-34/miR-449 for development and function to generate luminal turbulence. *Proc Natl Acad Sci USA* **116**, 3584–3593.

13 Mercey O, Popa A, Cavard A, Paquet A, Chevalier B, Pons N, Magnone V, Zangari J, Brest P, Zaragosi L-E *et al.* (2017) Characterizing isomiR variants within the microRNA-34/449 family. *FEBS Lett* **591**, 693–705.

14 Yuan S, Tang C, Zhang Y, Wu J, Bao J, Zheng H, Xu C and Yan W (2015) mir-34b/c and mir-449a/b/c are required for spermatogenesis, but not for the first cleavage division in mice. *Biol Open* **4**, 212–223.

15 Wu J, Bao J, Kim M, Yuan S, Tang C, Zheng H, Mastick GS, Xu C and Yan W (2014) Two miRNA clusters, miR-34b/c and miR-449, are essential for normal brain development, motile ciliogenesis, and spermatogenesis. *Proc Natl Acad Sci USA* **111**, E2851–E2857.

16 Comazzetto S, Di Giacomo M, Rasmussen KD, Much C, Azzi C, Perlas E, Morgan M and O'Carroll D (2014) Oligoasthenoteratozoospermia and infertility in mice deficient for miR-34b/c and miR-449 loci. *PLoS Genet* **10**, e1004597.

17 Wang L, Fu C, Fan H, Du T, Dong M, Chen Y, Jin Y, Zhou Y, Deng M, Gu A *et al.* (2013) miR-34b regulates multiciliogenesis during organ formation in zebrafish. *Development* **140**, 2755–2764.

18 Bao J, Li D, Wang L, Wu J, Hu Y, Wang Z, Chen Y, Cao X, Jiang C, Yan W *et al.* (2012) MicroRNA-449 and microRNA-34b/c function redundantly in murine testes by targeting E2F transcription factor-retinoblastoma protein (E2F-pRb) pathway. *J Biol Chem* **287**, 21686–21698.

19 Mercey O, Kodjabachian L, Barbry P and Marcet B (2016) MicroRNAs as key regulators of GTPase-mediated apical actin reorganization in multiciliated epithelia. *Small GTPases* **7**, 54–58.

20 Marcet B, Chevalier B, Coraux C, Kodjabachian L and Barbry P (2011) MicroRNA-based silencing of Delta/Notch signaling promotes multiple cilia formation. *Cell Cycle* **10**, 2858–2864.

21 Song R, Walentek P, Sponer N, Klimke A, Lee JS, Dixon G, Harland R, Wan Y, Lishko P, Lize M *et al.* (2014) miR-34/449 miRNAs are required for motile ciliogenesis by repressing cp110. *Nature* **510**, 115–120.

22 Lize M, Klimke A and Dobbelstein M (2011) MicroRNA-449 in cell fate determination. *Cell Cycle* **10**, 2874–2882.

23 Wildung M, Esser TU, Grausam KB, Wiedwald C, Volceanov-Hahn L, Riedel D, Beuermann S, Li L, Zylla J, Guenther A-K *et al.* (2019) Transcription factor TAp73 and microRNA-449 complement each other to support multiciliogenesis. *Cell Death Differ* **26**, 2740–2757.

24 Narita K, Nagatomo H, Kozuka-Hata H, Oyama M and Takeda S (2020) Discovery of a vertebrate-specific factor that processes flagellar glycolytic enolase during motile ciliogenesis. *iScience* **23**, 100992.

25 Forteza RM, Casalino-Matsuda SM, Falcon NS, Valencia Gattas M and Monzon ME (2012) Hyaluronan and layilin mediate loss of airway epithelial barrier function induced by cigarette smoke by decreasing E-cadherin. *J Biol Chem* **287**, 42288–42298.

26 Winkler GS (2010) The mammalian anti-proliferative BTG/Tob protein family. *J Cell Physiol* **222**, 66–72.

27 Delgehyr N, Meunier A, Faucourt M, Bosch Grau M, Strehl L, Janke C and Spassky N (2015) Ependymal cell differentiation, from monociliated to multiciliated cells. *Methods Cell Biol* **127**, 19–35.

28 Jain R, Pan J, Driscoll JA, Wisner JW, Huang T, Gunsten SP, You Y and Brody SL (2010) Temporal relationship between primary and motile ciliogenesis in airway epithelial cells. *Am J Respir Cell Mol Biol* **43**, 731–739.

29 Vladar EK and Brody SL (2013) Analysis of ciliogenesis in primary culture mouse tracheal epithelial cells. *Methods Enzymol* **525**, 285–309.

30 Cibois M, Luxardi G, Chevalier B, Thomé V, Mercey O, Zaragosi L-E, Barbry P, Pasini A, Marcet B and Kodjabachian L (2015) BMP signalling controls the construction of vertebrate mucociliary epithelia. *Development* **142**, 2352–2363.

31 Stuart T, Butler A, Hoffman P, Hafemeister C, Papalexi E, Mauck WM 3rd, Hao Y, Stoeckius M, Smibert P and Satija R (2019) Comprehensive integration of single-cell data. *Cell* **177**, 1888–1902.e21.

32 Wickham, H. (2009). ggplot2. https://doi.org/10.1007/978-0-387-98141-3

33 Nemajerova A, Kramer D, Siller SS, Herr C, Shomroni O, Pena T, Gallinas Suazo C, Glaser K, Wildung M, Steffen H *et al.* (2016) TAp73 is a central transcriptional regulator of airway multiciliogenesis. *Genes Dev* **30**, 1300–1312.

34 Kubo A, Yuba-Kubo A, Tsukita S, Tsukita S and Amagai M (2008) Sentan: a novel specific component of the apical structure of vertebrate motile cilia. *Mol Biol Cell* **19**, 5338–5346.

35 Fisch C and Dupuis-Williams P (2011) Ultrastructure of cilia and flagella – back to the future! *Biol Cell* **103**, 249–270.

36 Antoniades I, Stylianou P and Skourides PA (2014) Making the connection: ciliary adhesion complexes anchor basal bodies to the actin cytoskeleton. *Dev Cell* **28**, 70–80.

37 Yasunaga T, Wiegel J, Bergen MD, Helmstädter M, Epting D, Paolini A, Çiçek Ö, Radziwill G, Engel C, Brox T *et al.* (2022) Microridge-like structures anchor motile cilia. *Nat Commun* **13**, 2056.

38 Hoffman HK and Prekeris R (2022) Roles of the actin cytoskeleton in ciliogenesis. *J Cell Sci* **135**, jcs259030.

39 Lieb T, Forteza R and Salathe M (2000) Hyaluronic acid in cultured ovine tracheal cells and its effect on ciliary beat frequency in vitro. *J Aerosol Med* **13**, 231–237.

40 Huang TW, Cheng PW, Chan YH, Yeh TH, Young YH and Young TH (2010) Regulation of ciliary differentiation of human respiratory epithelial cells by the receptor for hyaluronan-mediated motility on hyaluronan-based biomaterials. *Biomaterials* **31**, 6701–6709.

41 Mano H, Nakatani S, Kimira Y, Mano M, Sekiguchi Y, Im RH, Shimizu J and Wada M (2015) Age-related decrease of IF5/BTG4 in oral and respiratory cavities in mice. *Biosci Biotechnol Biochem* **79**, 960–968.

42 Zheng W, Zhou Z, Sha Q, Niu X, Sun X, Shi J, Zhao L, Zhang S, Dai J, Cai S *et al.* (2020) Homozygous mutations in BTG4 cause zygotic cleavage failure and female infertility. *Am J Hum Genet* **107**, 24–33.

43 Pasternak M, Pfender S, Santhanam B and Schuh M (2016) The BTG4 and CAF1 complex prevents the spontaneous activation of eggs by deadenylating maternal mRNAs. *Open Biol* **6**, 160184.

44 Baran V, Brzakova A, Rehak P, Kovarikova V and Solc P (2016) PLK1 regulates spindle formation kinetics and APC/C activation in mouse zygote. *Zygote* **24**, 338–345.

45 Auer RL, Starczynski J, McElwaine S, Bertoni F, Newland AC, Fegan CD and Cotter FE (2005) Identification of a potential role for POU2AF1 and BTG4 in the deletion of 11q23 in chronic lymphocytic leukemia. *Genes Chromosomes Cancer* **43**, 1–10.

46 Stubbs JL, Vladar EK, Axelrod JD and Kintner C (2012) Multicilin promotes centriole assembly and ciliogenesis during multiciliate cell differentiation. *Nat Cell Biol* **14**, 140–147.

47 Funk MC, Bera AN, Menchen T, Kuales G, Thriene K, Lienkamp SS, Dengjel J, Omran H, Frank M and Arnold SJ (2015) Cyclin O (Ccno) functions during deuterosome-mediated centriole amplification of multiciliated cells. *EMBO J* **34**, 1078–1089.

Supporting information

Additional supporting information may be found online in the Supporting Information section at the end of the article.

Appendix S1. Supplemental methods.

Fig. S1. Expression of deuterosomal, multiciliated cell markers and *MIR34B/C* locus members during multiciliogenesis.

Fig. S2. *HOATZ*, *LAYN* and *BTG4* expression *in vivo* in human airway tissues from Human Cell Atlas data.

Fig. S3. *HOATZ* transcript expression is enriched in multiciliated cells of newborn pig airways, *in vitro* and *in vivo*.

Fig. S4. *HOATZ* isoform detection and ectopic expression.

Fig. S5. *BTG3* transcript expression is specific to human deuterosomal cells.

Fig. S6. Effect of *LAYN* silencing on multiciliogenesis.

Fig. S7. Schema illustrating HOATZ and LAYN protein localization in maturing (short cilia) and mature (long cilia) multiciliated cells (MCCs) in both human and mouse models.

Fig. S8. Uncropped Western blots.

Table S1. Single-cell correlation of gene expression of *HOATZ*, *FOXJ1* and *ENO4* in mTECs and HAECs.